Opt Quant Electron (2009) 41:921–932
DOI 10.1007/s11082-010-9406-y

On open boundary conditions for quantum cascade structures

G. Milovanovic · O. Baumgartner · H. Kosina

Received: 2 October 2009 / Accepted: 21 July 2010 / Published online: 6 August 2010

Abstract We present a study of tunneling current and an investigation of the optical gain of GaAs/$Al_{x_c}Ga_{1-x_c}$As quantum cascade lasers. Current carrying states are obtained by assuming Robin boundary conditions. Our simulation results show that this approach gives a very good agreement with other calculations using the Tsu–Esaki model and with simulations based on nonequilibrium Green's functions. By incorporating this method into optical gain calculations we establish good agreement with experimental results. Finally, the convergence of the solution of the Robin problem to the solution of the Dirichlet problem, as the energy tends to infinity, is investigated.

Keywords Quantum cascade laser · Robin boundary condition · Opticalgain current carrying state

1 Introduction

In 1970, Esaki and Tsu (1970) proposed using heterostructures for applications in optoelectronics. The first suggestion to use intersubband transitions in order to create a laser was made by Kazarinov and Suris (1971). Over the past several years, quantum cascade lasers (QCLs) have proven to be very promising candidates for practical sources of radiation, particularly in the midinfrared region (Gmachl et al. 2001).

Stationary transport of charge carriers in semiconductor devices is modeled by means of boundary value problems. In order to investigate systems with net current flows and obtain current-voltage characteristics of a quantum device, one has to impose boundary conditions which allow current carrying states. Homogeneous Neumann or Dirichlet boundary conditions yield a self-adjoint Hamiltonian matrix and cannot be used for open systems, since there is no interaction with the environment and the current density is identical zero (Kaiser et al. 2002). A popular approach is to assume periodic boundary conditions which ensure the

G. Milovanovic (✉) · O. Baumgartner · H. Kosina
Institute for Microelectronics, TU Wien, Gußhausstraße 27-29/E360, 1040 Wien, Austria
e-mail: milovanovic@iue.tuwien.ac.at

continuity of the current density, but in fact closes the system and makes the investigation of open system aspects impossible. The simulation domain is usually taken to be finite and the boundaries are physically given by device contacts. This leads to the necessity to consider open quantum systems with non-selfadjoint boundary conditions.

The focus of this work is on boundary conditions which yield current carrying states as solutions of the Schrödinger equation. The theoretical development is based on a Robin boundary condition approach when a solution with the Dirichlet boundary condition is available (Bondurant and Fulling 2005). A transformation converts a wave function satisfying a Dirichlet boundary condition to a wave function satisfying a Robin boundary condition, enabling particle exchange with the boundary. Within this scheme, the main focus of our work is to calculate the current density and the optical gain from the wave functions satisfying these boundary conditions. Comparing the results obtained with the proposed approach to other simulations and experimental measurements, we find that the concept of non-selfadjoint boundary conditions for the Schrödinger equation is satisfactory to QCL simulations.

In addition, we prove that the solution of the Robin problem converges to the solution of the Dirichlet problem, as the energy tends to infinity. Our results indicate the importance of considering adequate boundary conditions in determining fundamental properties of QCLs.

2 Theoretical framework

We consider electrons in the conduction band of a QCL in an electric field applied in the direction perpendicular to the heterointerfaces. The total wave function can be written as the product between the periodic Bloch function at the center of the Brillouin zone and an envelope function, which is supposed to vary slowly over one period. When z is the growth direction, the free motion in the in-plane direction can be separated and the envelope function in the quantum well structure is given by

$$\Psi_{i,k}(\mathbf{x}) = \frac{1}{\sqrt{A}} e^{i\mathbf{k}_\parallel \cdot \mathbf{x}_\parallel} \Phi_i(z) \tag{1}$$

where $\mathbf{k}_\parallel$ is the in-plane wave vector, A is the cross-sectional area of the quantum well structure, and $\Phi_i(z)$ is the electron envelope function of the ith state. Under the assumption that the periodic function is the same in all constituent parts and due to Eq. (1) the Schrödinger equation for the quantum well structure is given by

$$\left[-\frac{\hbar^2}{2} \frac{\partial}{\partial z} \frac{1}{\mathrm{m}^\star(z)} \frac{\partial}{\partial z} + \mathrm{V}_0(z) - eFz \right] \Phi_i(z) = E_i \Phi_i(z) \tag{2}$$

where E_i is the energy of the ith state, $\mathrm{m}^\star(z)$ denotes the effective mass, $\mathrm{V}_0(z)$ is the conduction band offset and F is the applied electric field.

Let $\Omega = [0, L]$ be the domain of the QCL perpendicular to quantum well layers. Assuming an incoming wave from $-\infty$ with amplitude 1 and no wave incident from $+\infty$, the Schrödinger equation can be solved explicitly outside the domain Ω

$$\Phi_i(z) = \begin{cases} e^{i\sqrt{2\mathrm{m}^\star E_i/\hbar^2}z} + R_i e^{-i\sqrt{2\mathrm{m}^\star E_i/\hbar^2}z}, & z < 0 \\ T_i e^{i\sqrt{2\mathrm{m}^\star (E_i - V)/\hbar^2}z}, & z > L \end{cases}$$

where $V(z) = 0$ on $(-\infty, 0)$ and $V(z) = V(L) = V_L < 0$ for $z > L$. We can deduce a boundary condition at $\partial\Omega \in \{0, L\}$ that does not involve reflection and transmission coefficients (Abdallah et al. 1997)

$$\hbar\Phi_i'(0) + i\sqrt{2\mathrm{m}^\star E_i}\Phi_i(0) = 2i\sqrt{2\mathrm{m}^\star E_i} \tag{3}$$

$$\hbar\Phi_i'(L) - i\sqrt{2\mathrm{m}^\star(E_i - V)}\Phi_i(L) = 0 \tag{4}$$

In order to construct a solution to the Schrödinger Eq. (2) with Robin boundary conditions when a solution to the same equation with Dirichlet boundary conditions is available, we make use of a Dirichlet-to-Robin transform (Bondurant and Fulling 2005). If $\Phi_{\mathrm{R}}(z)$ satisfies the Robin boundary condition at $\partial\Omega$

$$\frac{\partial}{\partial z}\Phi^{\mathrm{R}}(z)\big|_{\partial\Omega} - i\kappa\Phi^{\mathrm{R}}(z)\big|_{\partial\Omega} = 0 \tag{5}$$

the function

$$\Phi^{\mathrm{D}}(z) \equiv \frac{\partial}{\partial z}\Phi^{\mathrm{R}}(z) - i\kappa\Phi^{\mathrm{R}}(z) \tag{6}$$

corresponds to the solution of the Dirichlet problem, $\Phi^{\mathrm{D}}(z)\big|_{\partial\Omega} = 0$. For a given function $\Phi^{\mathrm{D}}(z)$, the general solution to the differential Eq. (6) can be written as

$$\Phi^{\mathrm{R}}(z) = e^{i\kappa z}\int_0^z e^{-i\kappa z'}\Phi^{\mathrm{D}}(z')dz' + Ce^{i\kappa z} \tag{7}$$

For the boundary condition (4) $\kappa = \sqrt{2\mathrm{m}^\star(E-V)/\hbar^2}$ and the constant C is evaluated by the requirement that $\Phi^{\mathrm{R}}(z)$ must satisfy the boundary condition (3) at $z = 0$. It is easy to see that

$$C = 2\frac{\tilde{\kappa}}{\tilde{\kappa} + \kappa} \tag{8}$$

where $\tilde{\kappa} = \sqrt{2\mathrm{m}^\star E/\hbar^2}$.

3 Optical gain

In QCLs intersubband transition contribute to the gain profile, especially the transition bewtween the lower and the upper laser level. In general, the standard expression for optical gain in semiconductors can be written as (Gelmont et al. 1996; Willenberg et al. 2003)

$$\mathrm{g}(\hbar\omega) = \frac{\pi e^2\hbar}{n\epsilon_0 c m_0^2\hbar\omega}|\mathrm{M}_{u,l}|^2\rho\int[\mathrm{f}_u(E) - \mathrm{f}_l(E)]\Lambda(\hbar\omega)dE \tag{9}$$

$\mathrm{f}(E)$ denotes the distribution function for the electrons. $|\mathrm{M}_{u,l}|^2$ represents the transition matrix element, ρ is the density of states, and Λ is the lineshape function. The E_i are quantized energies obtained by solving the Schrödinger equation. In a quantum well, the density of states can be taken as $\rho = \mathrm{m}^\star/\pi\hbar^2 L$ (Chang 2002) and the transition matrix element is approximated as the dipole matix element according to $\mathrm{M}_{u,l} = m_0^2\omega^2|z_{ul}|^2$. Substituting these approximations for the density of states and the dipole matrix element, and using the line shape as proposed in (Gelmont et al. 1996)

$$\Lambda(\hbar\omega) = \frac{\gamma(E)/\pi}{[\hbar\omega - E]^2 + \gamma^2(E)} \tag{10}$$

the optical gain can be estimated as (Cheung et al. 2000)

$$g(\hbar\omega) = \frac{e^2|z_{ul}|^2 m^\star \omega}{\hbar^2 c n_r \epsilon_0 L} \int_0^\infty dE \frac{\hbar\gamma(E)[f_u(E) - f_l(E)]}{\pi[\hbar\omega - E]^2 + [\hbar\gamma(E)]^2} \tag{11}$$

where z_{ul} is the dipole matrix element, n_r is the refractive index, ϵ_0 is the vacuum permittivity and c is the speed of light. The dipole matrix element depends strongly on the wave functions of the relevant states, and hence the optical gain itself. The validity of Eq. (11) is not restricted to any particular scattering mechanism. Certain assumptions have to be made about γ. We assume that the homogeneous broadening γ is dominated by the interaction with optical phonons (Gorfinkel et al. 1996). Thus

$$\gamma(E) = \gamma_0 \times \begin{cases} N_{ph} \\ (N_{ph}+1)\Theta(E - \hbar\omega_{ph}) \end{cases}$$

The top line describes optical phonon absorption and the bottom line optical phonon emission, where $\gamma_0 = (\pi e^2/2\hbar)[1/\varepsilon_\infty - 1/\varepsilon_0]q_{ph}$, $q_{ph} = (2m_e\omega_{ph}/\hbar)^{1/2}$, and the phonon occupation number is given by $N_{ph} = 1/(\exp(\hbar\omega_{ph}/k_BT) - 1)$. ε_0 and ε_∞ are the low and high frequency dielectric constants respectively.

4 Asymptotic behavior of the robin problem solution

Including a source term Q, we consider the most general effective mass Schrödinger equation in $\tilde{\Omega} := \Omega \setminus \partial\Omega$

$$\left[-\frac{\hbar^2}{2}\frac{\partial}{\partial x}\frac{1}{m^\star(x)}\frac{\partial}{\partial x} + (V(x) - E_i)\right]\Phi_i(x) = Q_i(x) \tag{12}$$

where Ω is the bounded domain with the boundary $\partial\Omega$. The corresponding Green's function is given by (Pozdeeva and Schulze-Halberg 2008)

$$G_{ij}(x,x') = -\frac{2}{c}\left[\Phi_i(x)\Phi_j^\dagger(x')\Theta(x-x') + \Phi_j(x)\Phi_i^\dagger(x')\Theta(x'-x)\right] \tag{13}$$

where Θ is the Heaviside function and c is a constant. Considering the Dirichlet boundary value problem

$$\Phi^D|_{\partial\Omega} = 0 \tag{14}$$

the solution for the effective mass Schrödinger equation at energy $E_i \in \mathbb{R}$ can be written in terms of the Green's function as follows

$$\Phi_i^D(x) = \int_{\tilde{\Omega}} G_{ij}(x,x')Q_j(x')dx' + \int_{\partial\Omega} G_{ij}(x,x')\Phi_j^D(x')dx' \tag{15}$$

The solution of the Robin boundary value problem

$$\frac{\partial}{\partial N}\Phi^R\big|_{\partial\Omega} - i\kappa\Phi^R\big|_{\partial\Omega} = 0 \tag{16}$$

converges to Φ^D as $E \to \infty$.

Proof Let

$$\tilde{\Phi}_i(x) := \int_{\tilde{\Omega}} \mathrm{G}_{ij}(x, x')\mathrm{Q}_j(x')dx' \tag{17}$$

Then $\Phi_i^{\mathrm{R}}(x) = \tilde{\Phi}_i(x) + \Phi_i^{\mathrm{T}}(x)$, where $\Phi_i^{\mathrm{T}}(x)$ satisfies

$$\hat{H}\Phi_i^{\mathrm{T}}(x) = 0 \qquad \text{in } \tilde{\Omega} \tag{18}$$

Due to the boundary condition (16) the following relation holds at the boundary

$$\left(\frac{\partial}{\partial N}\Phi_i^{\mathrm{T}} - i\kappa\Phi_i^{\mathrm{T}}\right)\Big|_{\partial\Omega} = -\left(\frac{\partial}{\partial N}\tilde{\Phi}_i - i\kappa\tilde{\Phi}_i\right)\Big|_{\partial\Omega} \tag{19}$$

In general, Φ_i^{T} can be written in the form

$$\Phi_i^{\mathrm{T}}(x) = \int_{\partial\Omega} \mathrm{G}_{ij}(x, x')\varphi_j(x')dx' \tag{20}$$

where φ can be determined by inserting Eq. (20) into the condition (19), which yields the following equation

$$\lim_{x\to\partial\Omega}\left(\int_{\partial\Omega}\left(\frac{\partial}{\partial N}\mathrm{G}_{ij}(x, x')\right)\varphi_j(x')dx' - i\kappa\int_{\partial\Omega}\mathrm{G}_{ij}(x, x')\varphi_j(x')dx'\right)$$
$$= \lim_{x\to\partial\Omega}\left(-\frac{\partial}{\partial N}\tilde{\Phi}_i(x) + i\kappa\tilde{\Phi}_i(x)\right)$$

Since $\kappa = O(\sqrt{E_i})$, we get

$$\lim_{x\to\partial\Omega}\int_{\partial\Omega}\mathrm{G}_{ij}(x, x')\varphi_j(x')dx' = \lim_{x\to\partial\Omega}\left(-\tilde{\Phi}_i(x) + O\left(\frac{1}{\sqrt{E_i}}\right)\right) \tag{21}$$

Inserting the Eqs. (14) and (15) yields

$$T_{ij}\varphi_j = T_{ij}\Phi_j^{\mathrm{D}} + O\left(\frac{1}{\sqrt{E_i}}\right) \tag{22}$$

where the operator T is defined as follows

$$T_{ij}\Phi_j(x') = \int_{\partial\Omega}\mathrm{G}_{ij}(\partial\Omega, x')\Phi_j(x')dx' \tag{23}$$

Thus,

$$\Phi_i^{\mathrm{R}}(x) = \tilde{\Phi}_i(x) + \int_{\partial\Omega}\mathrm{G}_{ij}(x, x')\Phi_j^{\mathrm{D}}(x')dx' + O\left(\frac{1}{\sqrt{E_i}}\right)$$
$$= \Phi_i^{\mathrm{D}}(x) + O\left(\frac{1}{\sqrt{E_i}}\right) \tag{24}$$

completing the proof. □

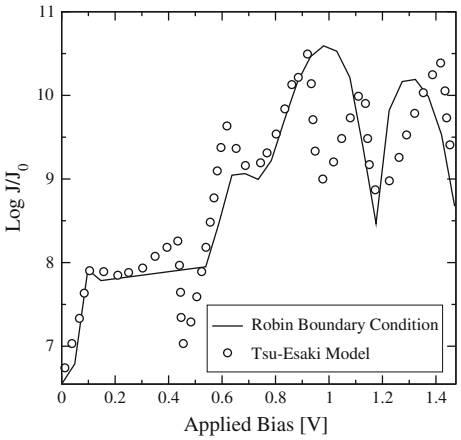

Fig. 1 Current-density voltage characteristics of a $GaAs/Al_{0.3}Ga_{0.7}As$ Fibonacci superlattice at $T = 200$K. The current density is scaled by $J_0 = Am^{-2}$

5 Results and discussion

On the basis of the Robin boundary conditions (3) and (4) the current density is numerically evaluated for periodic QCL structures as well for quasi-periodic systems. The transport of charge through the structure arises as a property of the wave function, and the current density is expressed as (Lee et al. 2006)

$$J_{(z)} = -\frac{2e}{A}\sum_{i,k_\parallel} f_i(k_\parallel)\mathrm{Re}\left[\Phi_i^\star(z)\frac{i\hbar}{m^\star(z)}\frac{\partial}{\partial z}\Phi_i(z)\right] \tag{25}$$

where A is the cross-sectional area of the quantum well structure. It has been shown that the electron distributions in both the active region and the injector subbands are thermalized and thus the energy distribution of electrons in each subband can be described by a Fermi-Dirac distribution function (Harrison 1999)

$$f_i(k_\parallel) = \frac{1}{1+\exp\left(\frac{E_i(k_\parallel)-E_{F,i}}{k_BT}\right)} \tag{26}$$

where $E_{F,i}$ is the quasi Fermi energy and $E_i(k_\parallel) = E_i + \hbar^2k_\parallel^2/2m^\star$. The electron states are evaluated within a selfconsistent Schrödinger-Poisson solver, where the electron concentration is related to the electronic wave functions and the electron sheet densities in the corresponding subbands which can be calculated according to the Fermi-Dirac distribution. For a given total sheet density the quasi Fermi level is obtained iteratively, where the initial value of the quasi Fermi level is taken to be $E_{F,i}(T) = E_c(T) - E_g(T)/2$ (Aspnes 1976), while the band gap is $E_g(T) = E_g(0) - 5.41[T^2/(T+204)10^{-4}]$ eV with $E_g(0) = 1.519 + 1.155x_c + 0.37x_c^2$ eV. The conduction band edge is given by $E_c(T) = E_g(T)$ for $0 \le x_c < 0.45$ and $E_c = E_X(T)$ for $x_c > 0.45$, where $E_X(T) = E_X(0) - 4.6[T^2/(T+204)10^{-4}]$ eV with $E_X(0) = 1.981 + 0.124x_c + 0.144x_c^2$ eV and the unit of the temperature is given in K.

Figure 1 compares the simulated current density using the Robin boundary condition approach with the current density calculated by the Tsu–Esaki model for a $GaAs/Al_{0.3}Ga_{0.7}As$ Fibonacci superlattice (FSL) (Panchadhyayee et al. 2008) which is a quasi-periodic multibarrier system. The FSL type considered has the sequence BBAB-BABBBABBABBBA, where A and B are the elementary blocks corresponding to the GaAs quantum well and the $Al_{0.3}Ga_{0.7}As$ barrier, respectively. The width of the well block is taken

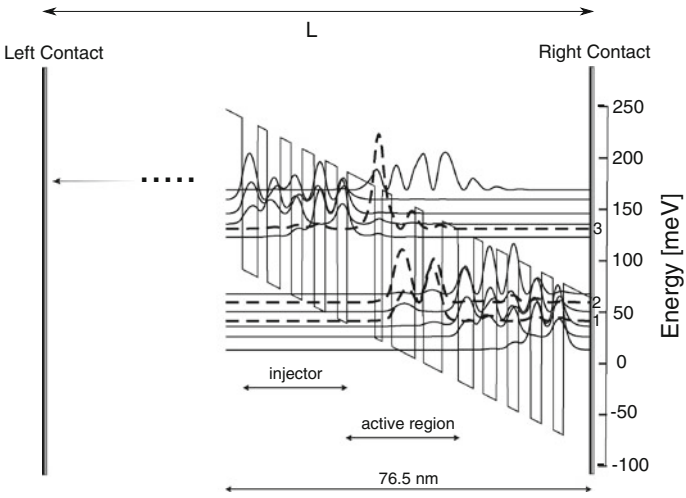

Fig. 2 A schematic diagram of the conduction band profile for one and a half periods of the $GaAs/Al_{0.33}Ga_{0.67}As$ QCL for an electric field of 48 kV/cm. The layer sequence of one period, in nanometers, is: **5.8**, 1.5, **2.0**, 4.9, **1.7**, 4.0, **3.4**, 3.2, **2.0**, 2.8, **2.3**, 2.3, **2.5**, 2.3, **2.5**, and 2.1, where *normal scripts* denote the wells and *bold* the barriers

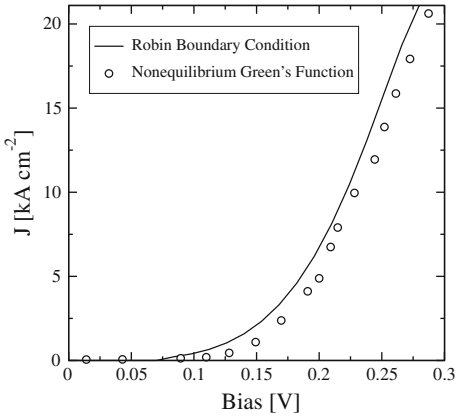

Fig. 3 Comparison of the current-voltage characteristic of a $GaAs/Al_{0.33}Ga_{0.67}As$ QCL calculated using the Robin boundary condition approach with a nonequlibrium Green's functions simulation

to be 5 unit cells, whereas the number of the unit cells for the barrier block equals to 3. The appearance of resonance-type peaks in the current density curves is typical for quasi-periodic systems, and the results obtained are in good agreement with the Tsu–Esaki model. The ability of the chosen boundary conditions to produce satisfactory current carrying states is also verified by comparing our results for the tunneling current density with calculations based on nonequilibrium Green's functions (Lee et al. 2006). For this purpose a typical example of a midinfrared quantum cascade laser is considered (Sirtori et al. 1998). Figure 2 illustrates the conduction band profile of this device. The comparison of the obtained current-voltage results with the simulation employing the nonequilibrium Green's functions method is illustrated in Fig. 3. The layer sequence of one period belonging to the $GaAs/Al_{0.33}Ga_{0.67}As$ structure, in nanometers, starting from the injection barrier is: **5.8**, 1.5, **2.0**, 4.9, **1.7**, 4.0, **3.4**, 3.2, **2.0**, 2.8, **2.3**, 2.3, **2.5**, 2.3, **2.5**, and 2.1, where normal scripts represent the wells, bold the barriers. The simulation is performed with the number of periods to be 30 and the temperature is taken

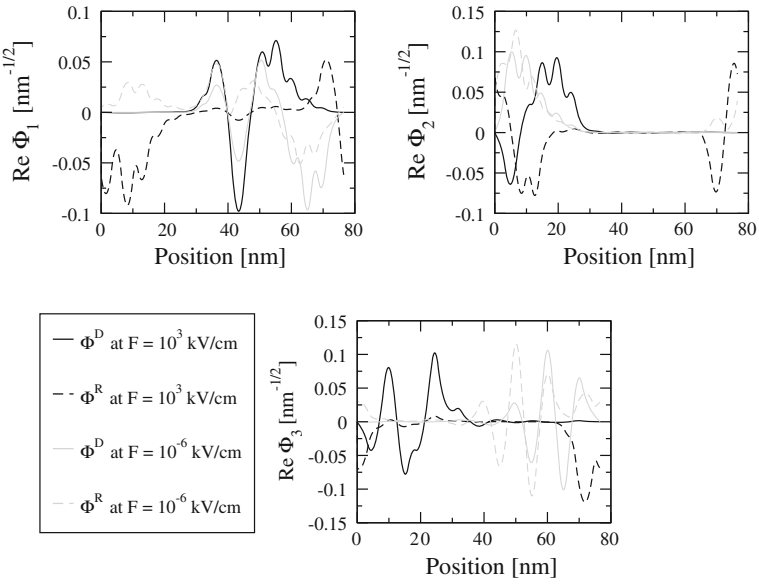

Fig. 4 The spatial dependencies of real components of the envelope functions are plotted for different values of the electric field. The *solid lines* correspond to the solution of the Dirichlet problem and the *dashed lines* represent the wavefunctions of the Robin problem

to be 77 K. As in the case of quasi-periodic superlattices, the application of our method to calculate current carrying states proves to be very promising for periodic QCL structures as well.

To illustrate the convergence of the solution to the Robin problem and the Dirichlet problem as $E_i \to \infty$, we investigated the transformations of the wave functions as a function of the applied electric field, because the energy levels increase as the electric field decreases. For this purpose the real part of the wave functions belonging to the Robin problem are compared to the solutions of the Dirichlet problem. The imaginary part, indicating the development of the current carrying states, are studied analogously. The order of magnitude we use for the electric field is 10^3 kV/cm on the one hand and 10^{-6} kV/cm for the weak field calculation. The investigated structure is the same three-level QCL design as above.

The real components of the wave functions are plotted in Fig. 4 for the electric fields $F = 10^3$ kV/cm and $F = 10^{-6}$ kV/cm. For $F = 10^3$ kV/cm the calculations show obvious deviations in the spatial dependence between the solutions of the Robin and Dirichlet boundary value problems, unlike the weak field case $F = 10^{-6}$ kV/cm, where a convergence between these solutions is observable[1].

The imaginary components of the wave functions corresponding to the Robin boundary value problem are plotted in Fig. 5. At the very small electric field $F = 10^{-6}$ kV/cm the imaginary wave function is almost zero everywhere except some very small peaks whose magnitudes are insignificant compared to the imaginary part of the wave function at $F = 10^3$ kV/cm.

Since the imaginary part of the wave function becomes zero with increasing energy, our results indicate that the tunneling current vanishes in this case. This behavior can be under-

[1] Although the applied bias of $F = 10^3$ kV/cm is not in the operation range of real devices, from a theoretical point of view the consideration of high fields is useful to demonstrate the region of the open nature in these structures.

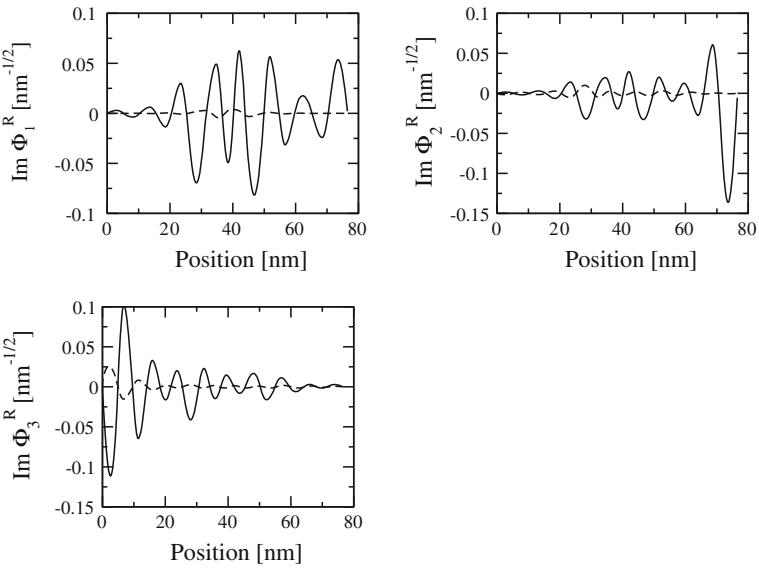

Fig. 5 The spatial dependencies of imaginary components of the envelope functions belonging to the solution of the Robin Problem at $F = 10^3$ kV/cm (*solid line*) and $F = 10^{-6}$ kV/cm (*dashed line*)

Table 1 Column one contains the applied electric fields in kV/cm

F	E_1	E_2	E_3	T(E_1)	T(E_2)	T(E_3)
10^3	9.7	11.4	24.4	0.683	0.721	0.787
10	31.5	49.8	67.8	0.524	0.611	0.672
10^{-2}	72.3	94.7	118.2	0.337	0.375	0.384
10^{-6}	114.6	138.8	169.3	0.118	0.133	0.171

The next three columns show the corresponding energy levels which are given in meV. Finally the transmission coefficients are given in the last three columns

stood in terms of the transmission coefficient which expresses the probability of tunneling and decays rapidly with energy according to (Mendez and Dominguez-Adame 1994)

$$\mathrm{T}(E) = \left(1 + \frac{V^2 \sinh^2(L\sqrt{2m^\star|V_L - E|/\hbar^2})}{4E(V_L - E)}\right)^{-1} \tag{27}$$

where T denotes the transmission coefficient for an electron in a heterostructure. As mentioned above, the energy levels increase as the electric field decreases. Due to Eq. (27) the transmission coefficient decreases significantly with decreasing electric field, which is illustrated in Table 1. The three energy levels correspond to the upper and lower laser levels.

Thus, by reducing the bias the conduction decreases and only minimal current flows. In this low field region the open boundary condition approach yields no significant deviation from the Dirichlet boundary value problem.

Finally, we focus on the calculation of optical gain under consideration of the proposed boundary conditions. Due to the strong dependence of the dipole matrix element on the wave function the determination of optical gain qualifies for verification of boundary conditions. We consider a laser that consists of 90 periods of a GaAs/$Al_{0.15}Ga_{0.85}$As heterostructure at

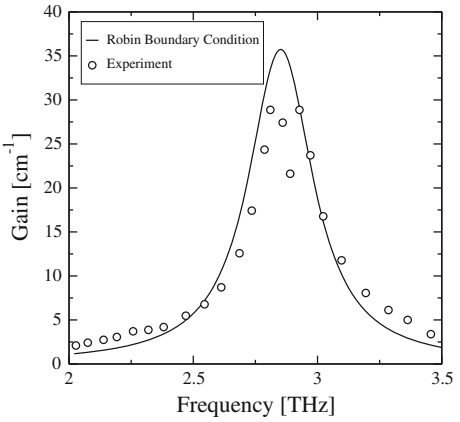

Fig. 6 Optical gain of a THz $GaAs/Al_{0.15}Ga_{0.85}$ As QCL driven at 160 A cm^{-2}. The *solid line* represents the result calculated by using the Robin boundary condition approach and the *dashed line* corresponds to measured values

a temperature of 70 K (Barbieri et al. 2004). The $GaAs/Al_{0.15}Ga_{0.85}As$ layer sequence in nanometers is **3.8**, 14.0, **0.6**, 9.0, **0.6**, 15.8, **1.5**, 12.8, **1.8**, 12.2, **2.0**, 12.0, **2.0**, 11.4, **2.7**, 11.3, **3.5**, and 11.6, where the AlGaAs layers are in bold. Figure 6 shows our simulation results to be in good agreement with measurements that are performed on this QCL design (Kröll et al. 2007).

The dipole matrix element between states Ψ_i and Ψ_j along the well growth direction z is given by (Coles et al. 1999)

$$z_{ij} = A\langle\Psi_i|z|\Psi_j\rangle = e^{i\mathbf{k}_\parallel\cdot\mathbf{x}_\parallel}\int_0^L z\Phi_i^\star(z)\Phi_j(z)dz \tag{28}$$

For numerical illustrations, $|\mathbf{x}_\parallel| \times \sphericalangle(\mathbf{x}_\parallel, \mathbf{k}_\parallel)$ is set to $2\pi/k_\parallel^{\max}$, and $k_\parallel^{\max} = 0.1$ nm^{-1}. The calculations of the dipole matrix elements, which where performed for two different values of electric fields F: 10^3 and 10^{-6} kV/cm, are illustrated in Fig. 7 as functions of the wave

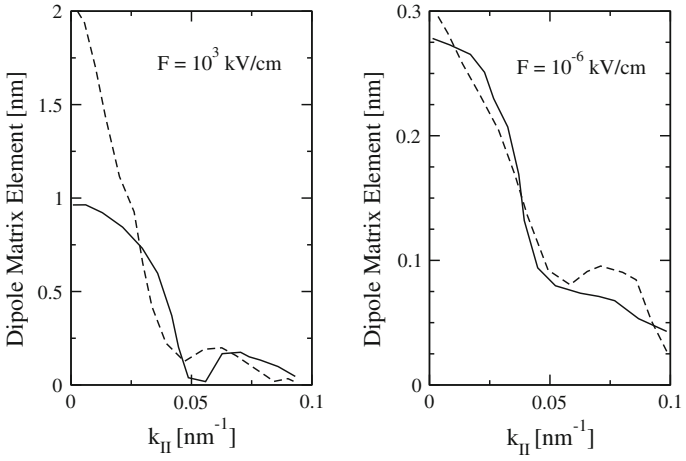

Fig. 7 Calculated values of the dipole matrix elements for $F = 10^3$ kV/cm and $F = 10^{-6}$ kV/cm. The *solid lines* represent the solution of the Dirichlet problem and the *dashed lines* correspond to the solution of the Robin problem

vector $k_\parallel$. The dashed curves represent the results determined taking into account Robin boundary conditions and the solid curves result from Dirichlet boundary conditions. A comparison of the results belonging to the different electric fields reveals that the solutions of the Robin and Dirichlet boundary value problems converge when lowering the electric field. Thus, our calculations demonstrate the accuracy of the proposed Robin boundary conditions for QCL simulations. However, for the unbiased case Dirichlet boundary conditions yield nearly comparable results.

6 Conclusion

We have presented numerical simulations of QCLs based on Robin boundary conditions. Special attention has been turned to calculations of the current density and optical gain which are fundamental parameters regarding the performance of a QCL. The method has been applied to several heterostructure designs, including a quasi-periodic Fibonacci superlattice. The results determined have been compared to simulations using nonequilibrium Green's functions and the Tsu–Esaki model and also experimental measurements. It has been found that good numerical agreement is obtained.

In addition, we have investigated the asymptotic behavior of the wave functions. A proof that the solution of the Robin problem converges to the solution of the Dirichlet problem has been presented. This behavior has been also illustrated numerically by comparing simulated wave functions as well as the dipole matrix elements of the Robin and Dirichlet boundary value problems in situations with high energy levels. It has been shown that the tunneling current is going to vanish with increasing energy, which can be explained in terms of the transmission coefficient.

Our results indicate the necessity to treat QCLs as open quantum systems with non-selfadjoint boundary conditions.

Acknowledgements This work has been supported by the Austrian Science Fund, special research program IR-ON (F2509).

References

Abdallah, N.B., Degond, P., Markowich, P.A.: On a one-dimensional Schrödinger-Poisson scattering model. ZAMP **48**, 135 (1997)

Aspnes, D.E.: GaAs lower conduction-band minima: ordering and properties. Phys. Rev. B **14**, 5331 (1976)

Barbieri, S., Alton, J., Beere, H.E., Fowler, J., Linfield, E.H., Ritchie, D.A.: 2.9 THz quantum cascade lasers operating up to 70 K in continuous wave. Appl. Phys. Lett. **85**, 1674 (2004)

Bondurant, J.D., Fulling, S.A.: The Dirichlet-to-Robin transform. J. Phys. A. Math. Gen. **38**, 1505 (2005)

Chang, W.S.C.: Principles of Lasers and Optics. Cambridge University Press, Cambridge (2002)

Cheung, C.Y.L., Rees, P., Shore, K.A., Pierce, I.: Self-consistent optical gain and threshold current calculations for near infrared intersubband semiconductor lasers. J. Mod. Optics **47**, 1857 (2000)

Coles, R.A., Abram, R.A., Brand, S., Burt, M.G.: Dipole matrix elements and the nature of charge oscillation under coherent interband excitation in quantum wells. Phys. Rev. B **60**, 13–306 (1999)

Esaki, L., Tsu, R.: Superlattice and negative differential conductivity in semiconductors. IBM J. Res. Dev. **14**, 61 (1970)

Gelmont, B., Gorfinkel, V.B., Luryi, S.: Theory of the spectral line shape and gain in quantum wells with intersubband transitions. Appl. Phys. Lett. **68**, 2171 (1996)

Gmachl, C., Capasso, F., Sivco, D.L., Cho, A.Y.: Recent progress in quantum cascade lasers and applications. Rep. Prog. Phys. **64**, 1533 (2001)

Gorfinkel, V.B., Luryi, S., Gelmont, B.: Theory of gain spectra for quantum cascade lasers and temperature dependence of their characteristics at low and moderate carrier concentrations. IEEE J. Quant. Electron **32**, 1995 (1996)

Harrison, P.: The nature of the electron distribution functions in quantum cascade lasers. Appl. Phys. Lett. **75**, 2800 (1999)

Kaiser, H.C., Neidhardt, H., Rehberg, J.: Density and current of a dissipative Schrödinger operator. J. Math. Phys. **43**, 5325 (2002)

Kazarinov, R.F., Suris, R.A.: Possibility of the amplification of electromagnetic waves in a semiconductor with a superlattice. Sov. Phys. Semicond. **5**, 707 (1971)

Kröll, J., Darmo, J., Dhillon, S.S., Marcadet, X., Calligaro, M., Sirtori, C., Unterrainer, K.: Phase-resolved measurements of stimulated emission in a laser. Nature **449**, 698 (2007)

Lee, S.C., Banit, F., Woerner, M., Wacker, A.: Quantum mechanical wavepacket transport in quantum cascade laser structures. Phys. Rev. B **73**, 245–320 (2006)

Mendez, B., Dominguez-Adame, F.: Numerical study of electron tunneling through heterostructures. Am. J. Phys. **62**, 143 (1994)

Panchadhyayee, P., Biswas, R., Khan, A., Mahapatra, P.K.: The effect of quasi-periodicity on the resonant tunneling lifetimes of states in electrically biased semiconductor superlattices. J. Phys. Condens. Matter **20**, 275, 243 (7 pp) (2008)

Pozdeeva, E., Schulze-Halberg, A.: Trace formula for Green's functions of effective mass Schrödinger equations and nth-order Darboux transformations. Int. J. Mod. Phys. A **23**, 2635 (2008)

Sirtori, C., Kruck, P., Barbieri, S., Collot, P., Nagle, J., Beck, M., Faist, J., Oesterle, U.: GaAs/$Al_xGa_{1-x}As$ quantum cascade lasers. Appl. Phys. Lett. **73**, 3486 (1998)

Willenberg, H., Doehler, G.H., Faist, J.: Intersubband gain in a Bloch oscillator and quantum cascade laser. Phys. Rev. B **67**, 85–315 (2003)